

*NW-12081
NASA CR-107142*

FINAL REPORT

(including STATUS REPORTS for

Periods December 1, 1967 - June 30, 1968

and July 1, 1968 - March 31, 1969)

**CASE FILE
COPY**

ORBITING ASTRONOMICAL OBSERVATORY

Contract NSR 03-002-048

(U. of A. Account No. 5603-920-245)

Principal Investigators

H. L. Johnson

T. Gehrels

Co-Investigators

F. A. deWiess

F. F. Forbes

Lunar and Planetary Laboratory

University of Arizona

Tucson, Arizona

June, 1969

This is the Final Report of work at the Lunar and Planetary Laboratory, University of Arizona, Tucson, Arizona under NASA Contract NSR 03-002-048 for the fourteen-month period ending June 30, 1968. It also represents the Status Reports for the periods December 1, 1967 to June 30, 1968 and July 1, 1968 to March 31, 1969. The following two proposal documents describe the effort for the Final Report period:

1. OAO-APT Program Plan, 14-month period (May 1, 1967 - June 30, 1968).
2. Addendum, OAO-APT Program Plan dated July 11, 1967.

These documents, References 1 and 2, respectively, are attached to this report, and they are outlined below.

OAO-APT Program Plan and Addendum

1. OAO Systems Studies
 - A. Mission Definition
 - B. Telescope Design
 - C. Fine Pointing
- II. Photopolarimeter Development
 - A. Optics
 - B. Data Handling
 - C. Configuration
- III. Fine Error Sensor Evaluation Program
 - A. Laboratory Tests
 - B. Telescope Use
- IV. Fourier Spectrometer Development Program
 - A. Configuration Design Study

V. Ground-Based Photometry Program

VI. Ground-Based Polarimetry Program

The results of work completed under the 14-month Program Plan are given in accordance with the above outline.

I. OAO SYSTEMS STUDIES

During the spring of 1967, the University of Arizona was invited to participate in a NASA program to draft scientific specifications for a man-attended, permanent, orbiting astronomical observing facility. The group of astronomers formed by NASA for this task was designated the "Astra Advisory Committee". As part of the OAO-Systems Studies F. F. Forbes participated in the Astra Committee and, together with R. E. Danielson of Princeton, prepared the Report of the Astra Advisory Committee, Ref. 3, attached to this report. The OAO Systems Studies work areas of Mission Definition, Telescope Design, and Fine Pointing are discussed in detail in this reference. The University of Arizona Experiment Package (AEP) is also presented in Ref. 3 (Appendix B-3) and is submitted to NASA as fulfilling the work outlined under Section I, OAO Systems Studies, in the OAO-APT Program.

II. PHOTOPOLARIMETER DEVELOPMENT

A. Optics

The optical configuration for the Arizona Experiment Package (AEP), is contained in Ref. 3 (Appendix B-3). In addition to filter photopolarimeters to obtain faint source ultraviolet measurements from 1050 Å to 5000 Å and moderate resolution multiplex spectroscopy from 1400 Å to 3500 Å, a high spatial resolution photometry system is described and is intended for operation in the 1600 Å to 6000 Å region. The latter capability would

be possible if the AEP were placed in orbit in an Astra Observatory on which diffraction-limited optics and precision pointing were employed. Use of man in the Astra program would extend the high resolution capability to photography and this is described in the AEP description (Ref. 3, Appendix B-3).

As part of the optics studies at the LPL, we have determined the birefringence of MgF_2 in the wavelength region 1299 \AA to 3000 \AA by combining our measurements of a Double Rochon Prism (Ref. 4) with the long wavelength index of refraction measurements made by R. Davis of the Smithsonian Astrophysical Observatory and T. Teska of the LPL. The results are presented for the first time in Figure 1 of this report. The index of refraction as a function of wavelength appears in Figure 2. As described in Ref. 4, we now have two ultraviolet polarization analyzers capable of performing on-axis polarization measurements from shortward of 1294 \AA to the visible wavelength region. The ultraviolet surface quality obtained with the Double Rochon Prism has been shown to be superb in that:

1. no absorptions occur in the birefringence measurements shown in Figure 1;
2. optical contact of elements in the ultraviolet has been achieved; and
3. the birefringence of MgF_2 , more than surface quality, determines the effectiveness of the material for use in the ultraviolet as a polarization analyzer.

Many of the optical elements to be used in a future AEP experiment require high quality ultraviolet reflective surfaces. We have examined

both the long term stability and ultraviolet surface quality of the highly stable, nickel coated, aluminum alloy Tenzaloy (Ref. 5). Contrary to reports of other cast aluminum alloys, such as 356T6 (Ref. 6), Tenzaloy has proven to be extremely stable and suitable for lightweight telescope optical systems. Reference 7, attached to this report, describes the performance of two telescopes which have 60-inch f/2 aluminum primary optics. In order to investigate further the stability of Tenzaloy, we fabricated during this reporting period two lightweight (15.8 lbs each) ribbed, 14 x 22 inch elliptical flats (see Fig. 3). With the exception of the choice of alloy these mirrors were identical to flats used previously in conjunction with the NASA Ames Convair 990 high-altitude program. While these Tenzaloy aluminum mirrors retain their two-wave figure as shown in Figure 4 (entire mirror surface) under all aircraft environment conditions, the two 356T6 aluminum mirrors which they replaced were found to have warped more than 200 wave within a 4-inch diameter.

Tenzaloy flats prepared as samples during this reporting period were also examined for surface quality. Through cooperation with Dr. H. E. Bennet of the Michelson Laboratory, the reflectance as a function of wavelength has been measured. According to Bennet, "If we assume that the distribution of surface irregularities is Gaussian, the rough surface should scatter normally incident light according to the relation $(R_0 - R)/R_0 = (4\pi\sigma/\lambda)^2$ where R is the amount of light the rough sample would reflect at normal incidence, R_0 is the reflectance of a perfectly smooth sample of the same material, and σ is the root mean square roughness. This relation can be used to calculate the scattered light as a function of wavelength for the 35 Å rms rough surface:

Wavelength (\AA)	R/R_0	$(R_0 - R)/R_0$
2000	0.9528	0.0472
5000	0.9923	0.0077
8000	0.9970	0.0030
10,000	0.9981	0.0019
20,000	0.9995	0.0005
50,000	0.9999	0.0001

Note that in the ultraviolet at 2000 \AA there is about 5% scattered light, but this amount decreases rapidly. In the near infrared at 8000 \AA there is only 0.3% scattered light, and there is even less at longer wavelengths."

B. Data Handling Processes

Under the present contract the data handling techniques employed with rapid scan polarimetry have been refined. The multichannel delay-line memory multiscaler previously reported (Ref. 8) has shown that multiscaling techniques are electronically feasible for the accumulation of rapid scan polarization data. During this reporting period, sufficient infrared polarization data were obtained on the objects listed in Table I to allow an extensive analysis of the rapid scan polarization approach. The data were recorded on magnetic tape, described previously (Refs. 9 and 10), and then multiscaled in the laboratory. The resulting punched paper tape was fed into an IBM 1130 computer and operated on by a two pass program, developed under the present contract, to compute the percentage polarization and phase angle for each star for each filter observed. In any future satellite containing Arizona ultraviolet polarimetry experiments, such computer programs would be used, either in the observatory or on the ground, to determine the polarization characteristics of observed objects. Approximately one-third of the infrared data has been processed to date, and sample preliminary infrared polarization results appear in Table II. This work will be completed under the present follow-on contract, and

papers describing the entire technique and results will be prepared at that time.

Additional studies for the use of multiscaling techniques have been applied to rapid scan spectra summation. The multiscaler is used to add repetitive spectra thereby suppressing noise introduced in any single scan. Reference 11, attached to this report, is a draft of a paper showing the effectiveness of the technique. The abstract for Ref. 11 follows:

An infrared spectrometer using a rotating, circular, variable-thickness interference filter has been used to obtain spectra of planets and late-type stars. The resolution of these spectra is of the order of 100.

These spectra seem to show a positive luminosity effect with respect to CO in normal M stars. Two Mira variables observed exhibit stellar steam absorption. NML Cygnus and NML Taurus show extremely red energy distributions and that of NML Cygnus may be essentially "flat" over the region covered by our observations.

C. Configuration Redefinition

The redefinition of the Arizona Experiment Package is presented in detail in Appendix B-3 of Ref. 3, the Report of the Astra Advisory Committee, referred to in the OAO System Studies section of this Report.

III. FINE ERROR SENSOR EVALUATION PROGRAM

The fine error sensor evaluation effort at the LPL under this contract has proven to be fruitful scientifically as well as technologically. Our extensive studies to optimize an observatory offset tracking design for the Arizona Experiment Package (AEP) were first reported in the Arizona Photopolarimeter Telescope (APT) Experiment Description of May 1965 and more recently in "Faint Star Tracking", Ref. 12, attached to this report. During this reporting period we have successfully used the offset tracker system, shown in Figure 5, to guide our 60-inch telescope in offset to

TABLE I

Object Observed				Filter Effective Wavelength			
				J 1.1 μ	H 1.65 μ	K 2.25 μ	L 3.5 μ
NML Cygnus	CIT 6	α Boo	CIT 9	x	x	x	x
β Peg	VCV n	R Leo	CIT 11	x	x	x	x
β And	δ Per	CIT 7	CIT 12	x	x	x	x
α Tau	+ 31 1049	CIT 8	μ Cep	x	x	x	x
α Ori	+ 32 1109	δ Oph	μ UMa	x	x	x	x
β Gem	Mars	g Her	NML Tau	x	x	x	x
ω Cet	Venus	α Her		x	x	x	x
α Ari	BS 2289	CIT 3	ν Sag	x	x	x	
β Peg	BS 2190	CIT 5	α Hya	x	x	x	
α Per	RS Cnc	α Gem		x	x	x	
83 UMa	Mercury						x
CIT 10					x	x	x
54 Leo	R CrA	BS 6242	θ CrB		x		
δ Boo	α CrA	ξ^2 Sgr	ϵ Her		x		

TABLE II. Sample Preliminary Polarization Results

Filter	% P	σ	Filter	%P	σ
<u>NML Cygnus</u>			<u>Standard Stars</u>		
J	4.95	.77	<u>α Ori (Jan 67)</u>		
H	3.00	.26	J	.15	.21
K	4.1	.5	H	.23	.21
L	1.3	.4	K	.30	.22
<u>NML Taurus</u>			<u>α Ori (Feb 67)</u>		
J	.91	.20	J	.27	.14
H	.91	.12	H	.15	.11
K	.49	.22	K	.15	.16
<u>VCVn</u>			<u>R Leo (Jan 67)</u>		
J	.98	.13	J	.36	.25
H	.43	.13	H	.18	.13
K	.17	.18	K	.13	.15
<u>CIT 6 (Jan 67)</u>			<u>R Leo (Feb 67)</u>		
J	1.70	1.24	J	.17	.09
H	1.87	.22	H	.15	.11
K	1.15	.15	K	.06	.18
<u>CIT 6 (Feb 67)</u>			<u>μ UMa</u>		
J	2.32	1.60	J	.09	.19
H	1.73	.29	H	.18	.16
K	1.17	.25	K	.20	.15
<u>Mars (Jan 67)</u>			<u>β And</u>		
J	1.28	.16	J	.11	.14
H	2.12	.17	H	.26	.20
K	2.45	.23	K	.28	.16
<u>Mars (Feb 67)</u>			<u>α Tau (Dec 66)</u>		
J	.61	.10	J	.72	.16
H	1.05	.10	H	.78	.15
K	1.50	.17	K	.42	.18
<u>Venus (Feb 67)</u>			<u>α Tau (Jan 67)</u>		
J	1.40	.14	J	.35	.10
H	.89	.25	H	.10	.10
K	.98	.23	K	.10	.20
<u>δ Per</u>					
J	2.23	.13			
H	1.04	.12			
K	.69	.15			
<u>+31 1049 (Jan 67)</u>					
J	.42	.14			
H	.72	.14			
K	.03	.14			
<u>+31 1049 (Feb 67)</u>					
J	.26	.12			
H	.62	.09			
K	.55	.22			

obtain infrared polarization and interferometric data. Also, F. F. Forbes participated in a NASA-ERC project to generate a Design Criteria Monograph on space-borne star trackers. While this work was at no expense to this contract, two significant papers, (References 13 and 14), resulted which greatly simplify the determination of star characteristics when used as star tracker targets. The abstract for the more extensive of these two papers, Ref. 14, is as follows:

The photodetector responses to the radiant energy incident on the Earth's atmosphere from the 964 brightest stars north of declination -20° are presented for the S-1, 4, 11, 17, and 20 and Bialkali photocathode materials and for the silicon detector. The computations for these data are based on recent Lunar and Planetary Laboratory 13-color narrow-band filter photometry. Photodetector response data for 67 navigational stars, based on existing UBVRIJ photometry for stars south of declination -20° , are also included.

A. Laboratory Tests

We have used test systems of the fine error sensor (see Figure 6) to demonstrate successfully in the laboratory that targets generating only a few photoelectrons per second at the tracker image dissector anode may be tracked. This result is shown in the photographs of Figure 7. The laboratory system shown in Figure 6 has been used to simulate the observatory closed-loop system in that a mechanical connection was made between the micrometer stage, which positions an artificial star, and the telescope drive motor shaft. This technique has proven useful not only because it allows us to check the entire system under closed-loop laboratory conditions but also because it affords an opportunity to optimize dynamically system time constants. The laboratory test system was also used to test our spiral acquisition scan design. The design and test results of the acquisition system are presented in Ref. 15 of this report.

B. Telescope Use

The offset guider, shown in Figure 5 attached to an LPL 60-inch telescope, has been used continuously as the prime telescope drive source for offset operation. That is, a photometer or interferometer placed at the focal plane of the 60-inch telescope has been able to measure nearly invisible objects, such as the NML Cygnus object, when the tracker was provided the right ascension and declination drive signals for the telescope from signals from another star, off-axis from the NML Cygnus object and bright enough to track in the visible. Further, the tracker has been used to provide error signals to drive the telescope for precise interferometer measurements of the planet Venus by modifying the track scan so that it extends just beyond the illuminated crescent of the planet. The tracking accuracy seems to be seeing limited for tracking Venus as it is for stellar targets.

Finally, the tracker has been used in the following unique manner: When the image dissector gain is reduced, the tracker is capable of generating suitable telescope drive error signals from specific features on the lunar surface in a way not unlike that of tracking either a faint star surrounded by a faint-star background or a bright star during full-day light. In all three cases the tracker centers upon the light centroid, and the only requirement is that some contrast exist in the region scanned by the track scan. While using the tracker as a lunar feature tracker, we have observed the following characteristics:

1. There are probably over 100 suitable features on the lunar surface at full moon which will allow direct or offset tracking to an accuracy of better than 1 sec (approximate seeing limit) - providing, therefore, precise direct lunar tracking.

2. The tracker prefers features away from the terminator toward the bright limb so that shadow motion or apparent bright feature motion near the terminator is of no consequence.
3. An illuminated crater rimlet of a small crater appears to the tracker as a small planet near crescent phase and provides an excellent track error signal.
4. The lunar feature tracker performs as well during Earth day as it does at night because it senses feature-to-background contrast only. However, dust flecks on the tracker optics can give very pronounced signals. These signals have reversed logic and are rejected. Reversing the logic would allow us to check the system stability and to track on a dark feature.
5. When the tracker is directed toward the Moon and turned on, it hunts in a pin-ball machine fashion for a suitable target. If it is too near the bright limb where no target exists, it will drift toward the limb and run around, until a bright limb feature is found.

In conclusion, a wobble system has been installed in the tracker which allows specific offsets to be inserted so that the telescope can be automatically accurately positioned between two adjacent portions of sky. This is particularly useful for double beam infrared photometry and interferometry.

IV. FOURIER SPECTROMETER DEVELOPMENT PROGRAM

The effectiveness of a multiplex spectrometer in an observatory satellite or at a ground-based observatory depends on the following two properly designed and fabricated items:

1. Multiplex spectrometer optimized for desired wavelength range resolution and environment.
2. Suitable means to acquire, store, and process interferograms which, when properly operated upon in the computer, will yield spectra with the desired resolution over the wavelength range selected.

During this reporting period we have studied both areas in depth, with the result that we now possess at the LPL the necessary working computer programs to generate high quality spectra suitable for publication. We have investigated two multiplex spectrometer designs that would be capable of obtaining ultraviolet spectra.

A. Configuration Design Study.

One possible configuration for a Fourier Spectrometer appears in Ref. 3 (Appendix B-3). Optical schematics for this Fourier Spectrometer are shown in Figures 8a and 8b. The resolution is designed to be less than 100 cm^{-1} in the wavelength range from 1400 \AA to 3500 \AA . The anticipated resolution as a function of wavelength is presented in Figure 9 where the resolution is shown to be approximately 55 cm^{-1} at 1770 \AA and is better than 2 \AA from about 1450 \AA to 1950 \AA .

In an effort to increase spectrometer transmission and resolution, we have also examined the extension of the Michelson interferometer into the ultraviolet wavelengths. The design which was considered is shown in Figure 10. Although prism spectrometers similar to that shown in Figures 8a and 8b have been successfully fabricated for the visible and near ultraviolet wavelengths, the Michelson interferometer appears to hold the most potential for use in the ultraviolet. Our studies indicate that a resolution of 10 to 20 cm^{-1} is attainable. This is competitive with instruments of comparable resolution and there is a further advantage in that for the most part reflective optics may be used. Considerable effort will be needed to extend the usefulness of the spectrometer into the vacuum ultraviolet; specifically, an appropriate ultraviolet beam splitter must be devised. The principal advantage of the interferometer shown in Figure 10 is that the beam splitters are interchangeable and this allows the various interfero-

meter elements to be studied independently. The fabrication and testing of this device will be the primary objective of our follow-on effort at the LPL.

It should be noted that our interferometric program has been delayed by eight months because funds due July, 1968 did not arrive until March, 1969. However, an interferometer has now been purchased and its expected arrival date is September 1, 1969.

We have been successful in measuring infrared stellar spectra with a Michelson interferometer not purchased under this contract. The optical schematic for this 8 cm^{-1} resolution PbS instrument is shown in Figure 11 and a photograph appears in Figure 12. With this device we have identified the critical elements in a Michelson interferometer that must be perfected for ultraviolet use. In addition to using this interferometer to study the techniques in practical stellar interferometry, we have obtained significant scientific data. Three publications, References 16, 17, and 18, attached to this report and with abstracts below, represent work that was supported in part by this contract and this was acknowledged in the papers.

Reference 16

ABSTRACT

The human eye senses only a small fraction of the total energy reaching our planet from distant objects. Moreover, the radiation in the infrared wavelengths longer than those seen by the eye is partially blocked by our atmosphere; and the shorter ultraviolet wavelengths cannot be detected by even the most sensitive ground-based instruments. However, there are 'windows' in the infrared through which astronomical objects can be viewed with specialized equipment. Already the existence of very cool stars, possibly protostars or preplanetary systems in the process of formation, has been suggested by infrared astronomers who have discovered objects that are relatively bright in the infrared but extremely faint in the visible wavelengths. Infrared techniques may also shed light on those powerful sources of radiation known as quasars. In 1964 one of us (Johnson) made the first recording of the infrared emission from quasar 3C 273 and found it to be in excess of that expected - an observation which like so many in the field of quasars remains so far unexplained.

Reference 17

ABSTRACT

We have made infrared spectroscopic observations of 21 stars, using a rapid-scanning Michelson interferometer. The range of wavelength is from 1.2μ (8200 cm^{-1}) to 2.6μ (3900 cm^{-1}), and the resolution is 8 cm^{-1} . All spectra have been corrected for atmospheric extinction, mostly by the method of equal-altitude photometric transfers from standard objects. The atmospheric transmission corrections are based upon a Lunar spectrum obtained from the NASA Convair 990 Jet Aircraft, at an altitude of 41,500 feet. The corrected ground-obtained spectrum of α Ori was checked by an aircraft spectrum of the same star, showing that the extinction corrections are valid.

Only four stars, all Mira variable stars, showed significant amounts of steam absorption in their spectra. There exists a correlation of this absorption with long-wavelength ($9\text{-}14 \mu$) infrared excess for giant stars, but not for supergiants.

Reference 18

ABSTRACT

An infrared spectrum from 1.4μ (7000 cm^{-1}) to 4.0μ (2500 cm^{-1}) has been obtained for the NML Cygnus infrared star. A rapid-scanning Michelson interferometer was used. The structure of the CO bands around 4300 cm^{-1} indicates a temperature of 2000° K . As before, a large infrared excess, compared to those of giants of the same temperature, was found. A broad absorption at 3300 cm^{-1} (3.03μ) was found; this absorption may be due to interstellar ice.

V. GROUND-BASED PHOTOMETRY PROGRAM

The Status Report for the period May 1, 1967 to November 30, 1967 outlines the progress made in the ground-based photometry program during that interval of time. At the request of NASA this program was curtailed after November 30, 1967 because of a lack of funds. Fortunately, it was possible to complete the work with funds from the National Science Foundation. The results are contained in Ref. 19, "Thirteen-Color Narrow-Band Photometry of One Thousand Bright Stars", in which the support of

NASA is acknowledged. The abstract of Ref. 19 follows:

In this report our previously published eight-color photometry, obtained with a RCA 1P21, is combined with new red-infrared photometry obtained with a RCA 7102. The final system of thirteen colors provides two sample points in the continuum above the Balmer discontinuity and two points below; similarly it gives four sample points above the Paschen discontinuity. The wavelength range of the photometry extends from 0.33 to 1.10 μ . We have derived from recent literature an absolute energy calibration for the thirteen-color photometry.

VI. GROUND BASED POLARIMETRY PROGRAM

The progress made in the ground-based polarimetry program from May 1, 1967 to November 30, 1967 is contained in the Status Report covering that period of time. After November 30, 1967 it was necessary to curtail this work, at NASA's request, because of a lack of funds; and no additional papers have been published.

REFERENCES

1. OAO-APT Program Plan (1 May 67 - 30 June 68).
2. Addendum, OAO-APT Program Plan, dated 11 July 1967.
3. Report of the Astra Advisory Committee, July 1968.
4. "A Polarizer for the Vacuum Ultraviolet", Applied Optics 6, No. 6, June 1967, (D.L. Steinmetz, W.G. Phillips, M. Wirick, and F.F. Forbes).
5. Tenzaloy is an aluminum alloy produced by the American Smelting and Refining Co. It is composed of 7.5% zinc, 0.6% copper, 0.4% magnesium, and the balance aluminum.
6. S.P. Maran, paper presented at 124th meeting of the American Astronomical Society at Williams Bay, Wisconsin (1967).
7. F.F. Forbes, "Large Aperture Aluminum Alloy Telescope Mirrors", Applied Optics, 7, July 1968.
8. "Multichannel Delay-Line Memory for Scientific Data Accumulation", XIII Rassegna Internazionale Electronica e Nucleare, Rome, 835, June 1966, F.F. Forbes.
9. "The Infrared Polarization of the Moon", Communications of the Lunar and Planetary Laboratory, No. 113, 9 November 1967, (F.F. Forbes and P.A. Welch).
10. "The Infrared Polarization of the Infrared Star in Cygnus", The Astrophysical Journal, 147, No. 3, March 1967, (F.F. Forbes).
11. "Stellar and Planetary Spectra in the Infrared from 1.35 μ to 4.10 μ ", 17 March 1969, (F.F. Forbes, W. Stonaker, and H.L. Johnson), in press.
12. "Faint Star Tracking", 3 September 1968, (F.F. Forbes).

REFERENCES (continued)

13. "Stellar Photometric Data for Various Photocathode Materials",
Applied Optics, March 1969, (F.F. Forbes and R.I. Mitchell).
14. "Stellar Photometric Data for Six Different Photocathode Materials
and the Silicon Detector", Communications of the Lunar and Planetary
Laboratory, No. 142, 15 December 1968, (F.F. Forbes and R. I. Mitchell).
15. Spiral Acquisition Scan System.
16. "Infrared Astronomy", Science Journal, April 1968, (F.F. Forbes and
H.L. Johnson).
17. "Stellar Spectroscopy, 1.2 μ to 2.6 μ ", Communications of the Lunar and
Planetary Laboratory, No. 113, August 1968, (H.L. Johnson, I. Coleman
R.I. Mitchell, and D.L. Steinmetz).
18. "The Infrared Spectrum of the NML Cygnus Object", Ap. J., Vol. 154,
December 1968, (H.L. Johnson).
19. Thirteen-Color Narrow-Band Photometry of One Thousand Bright Stars",
Communications of the Lunar and Planetary Laboratory, No. 132, February
1969, (R.I. Mitchell and H.L. Johnson).

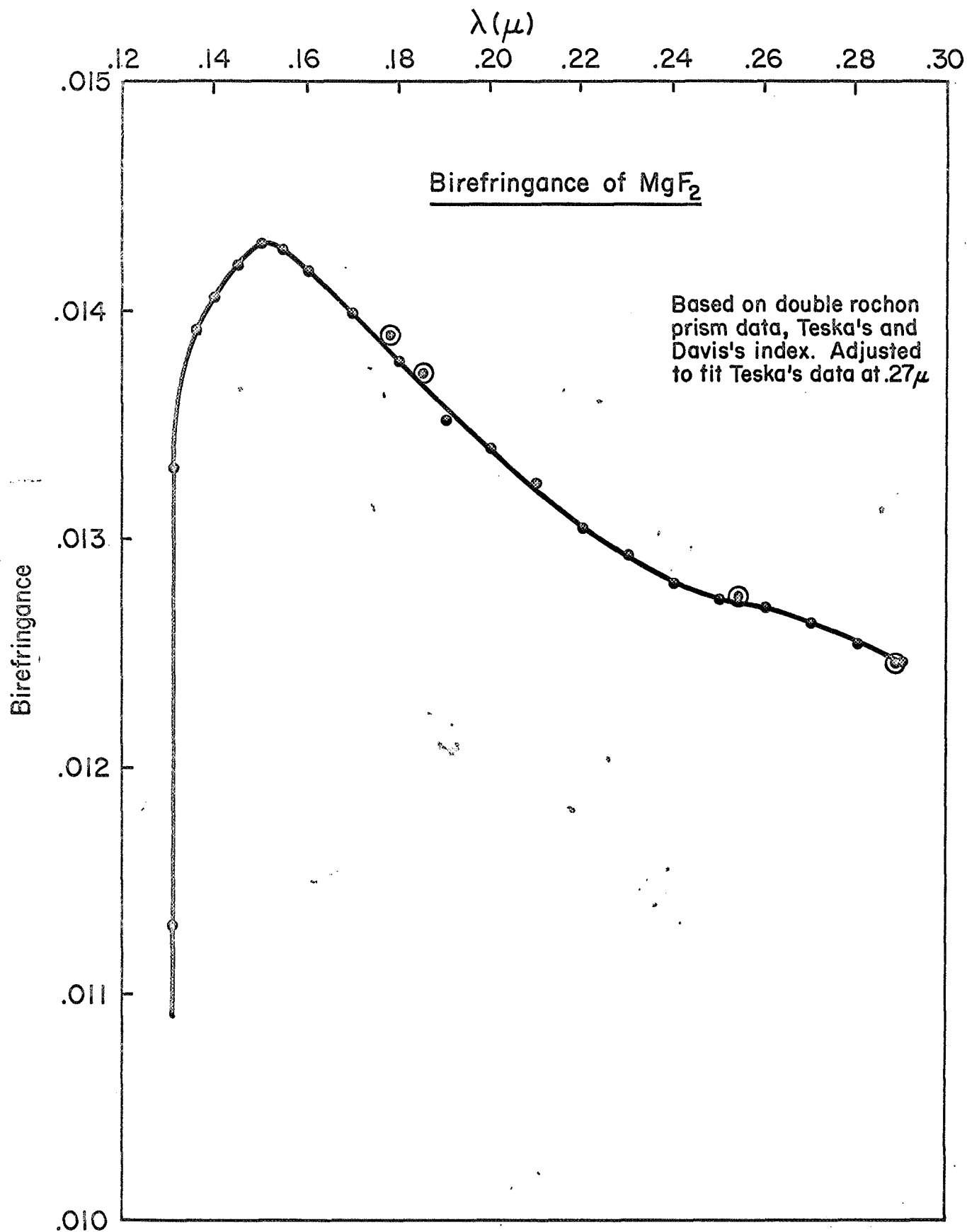


Figure 1.

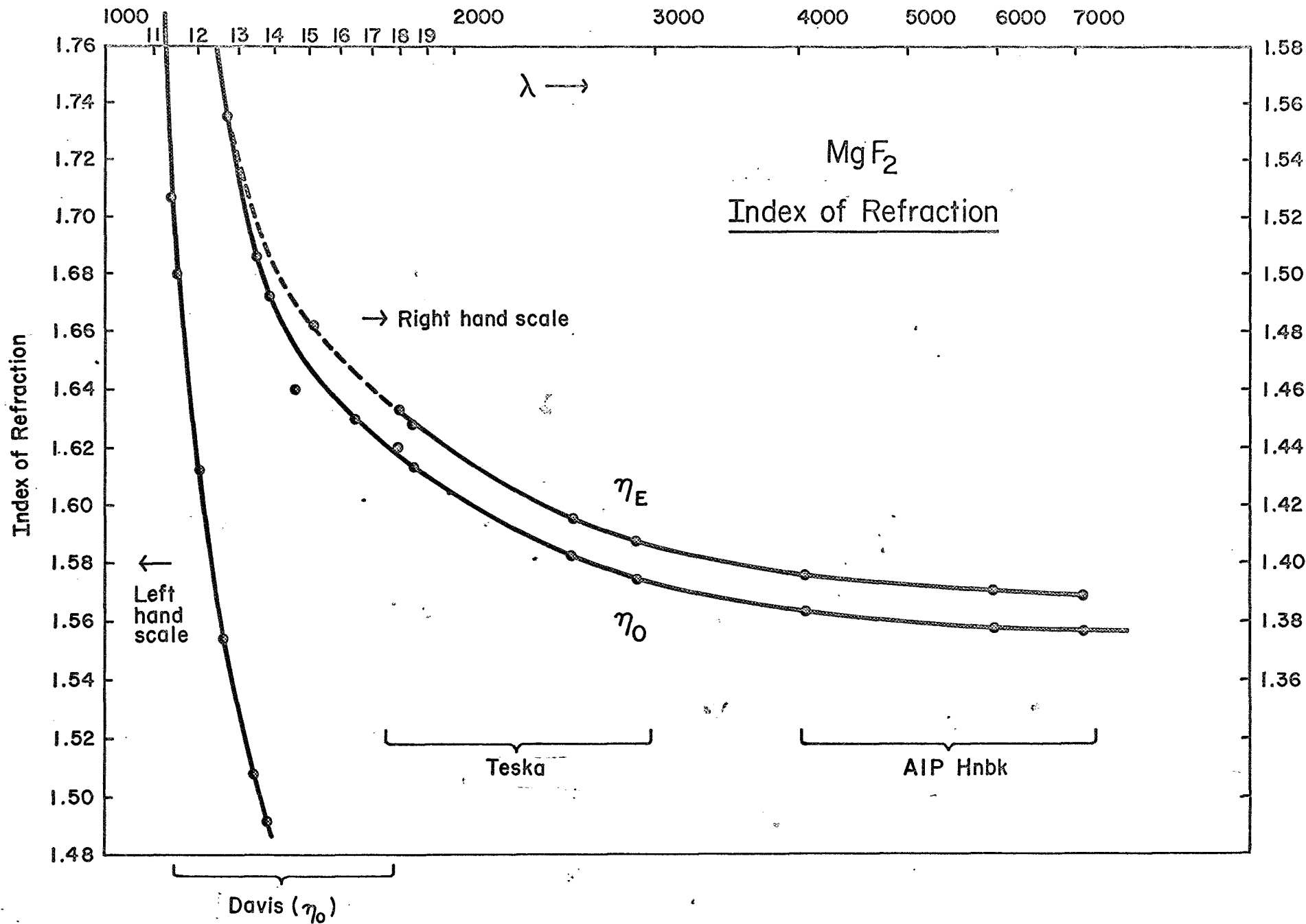


Figure 2.

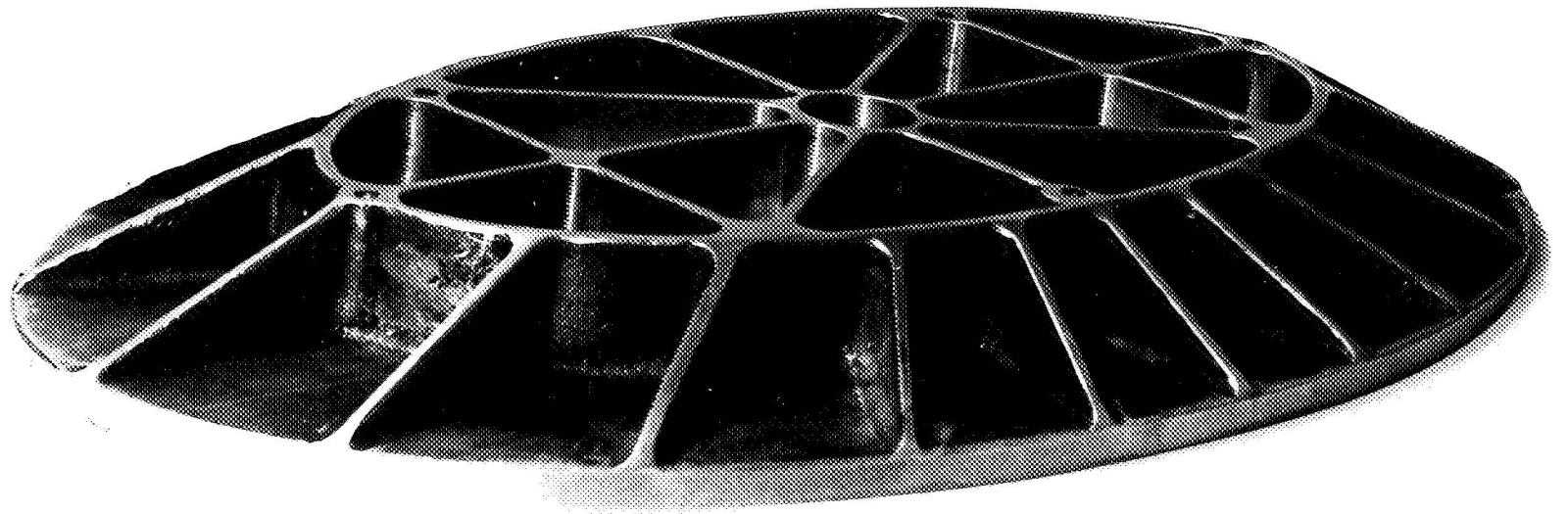
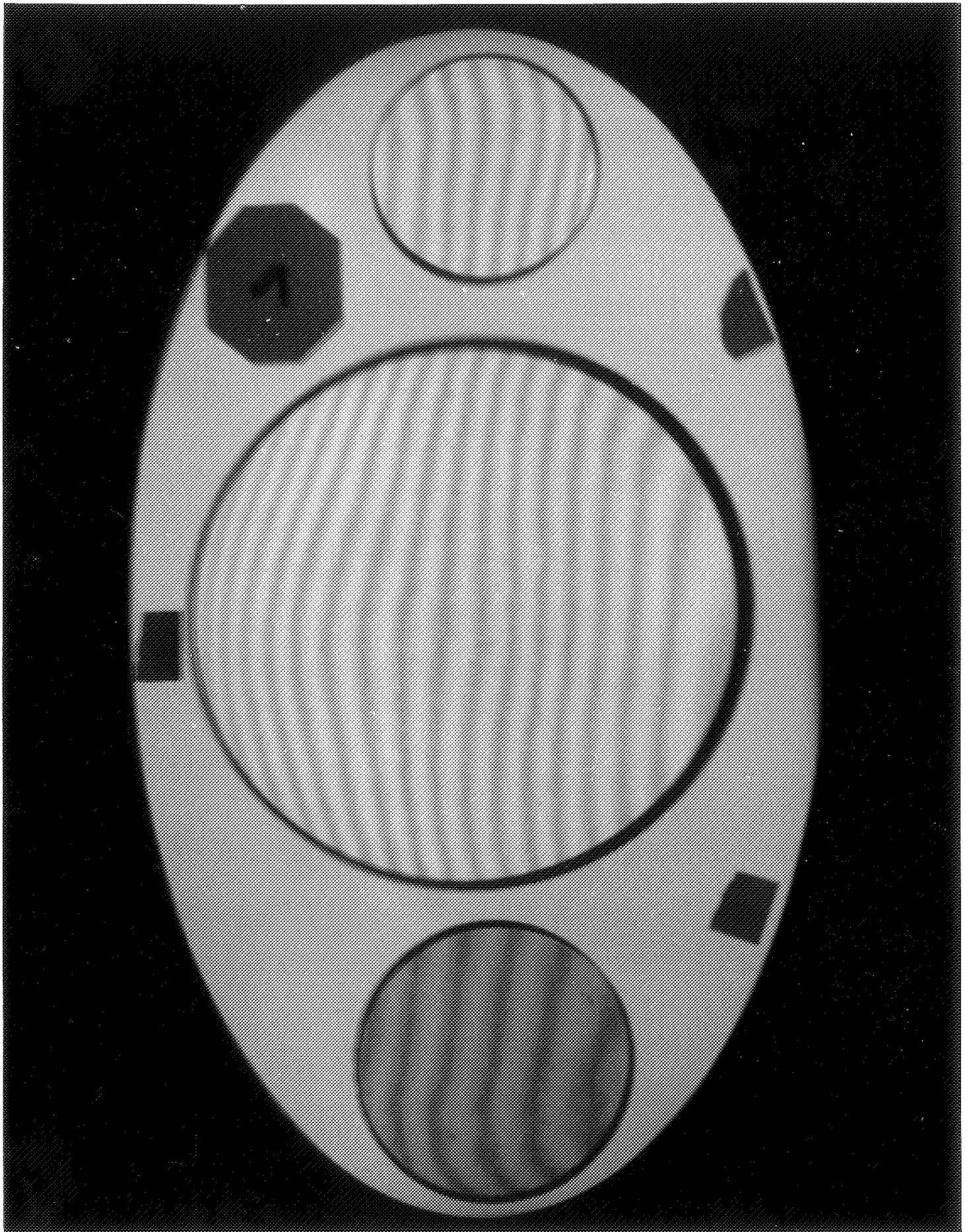


Fig. 3



4.1.1

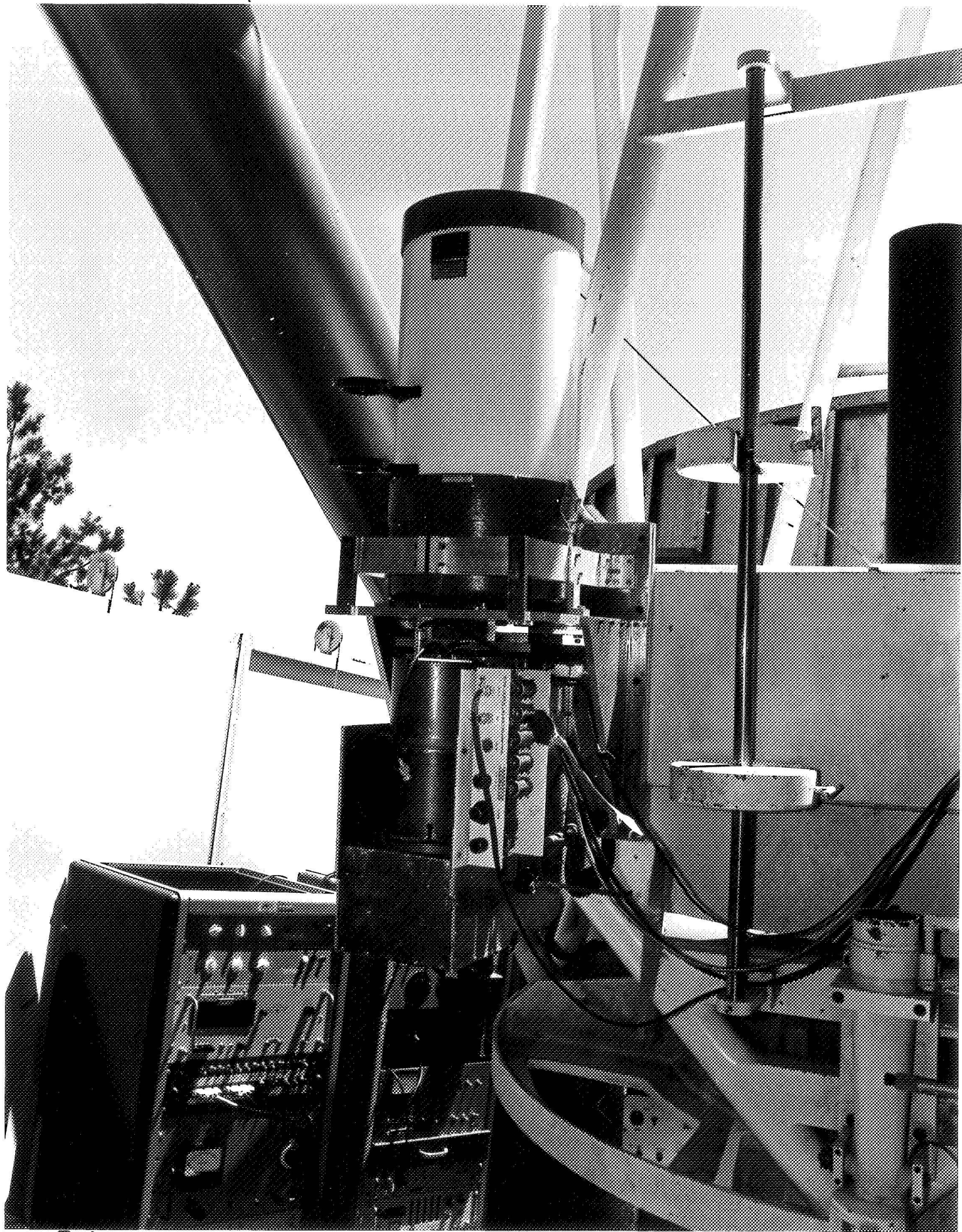


Fig. 5.

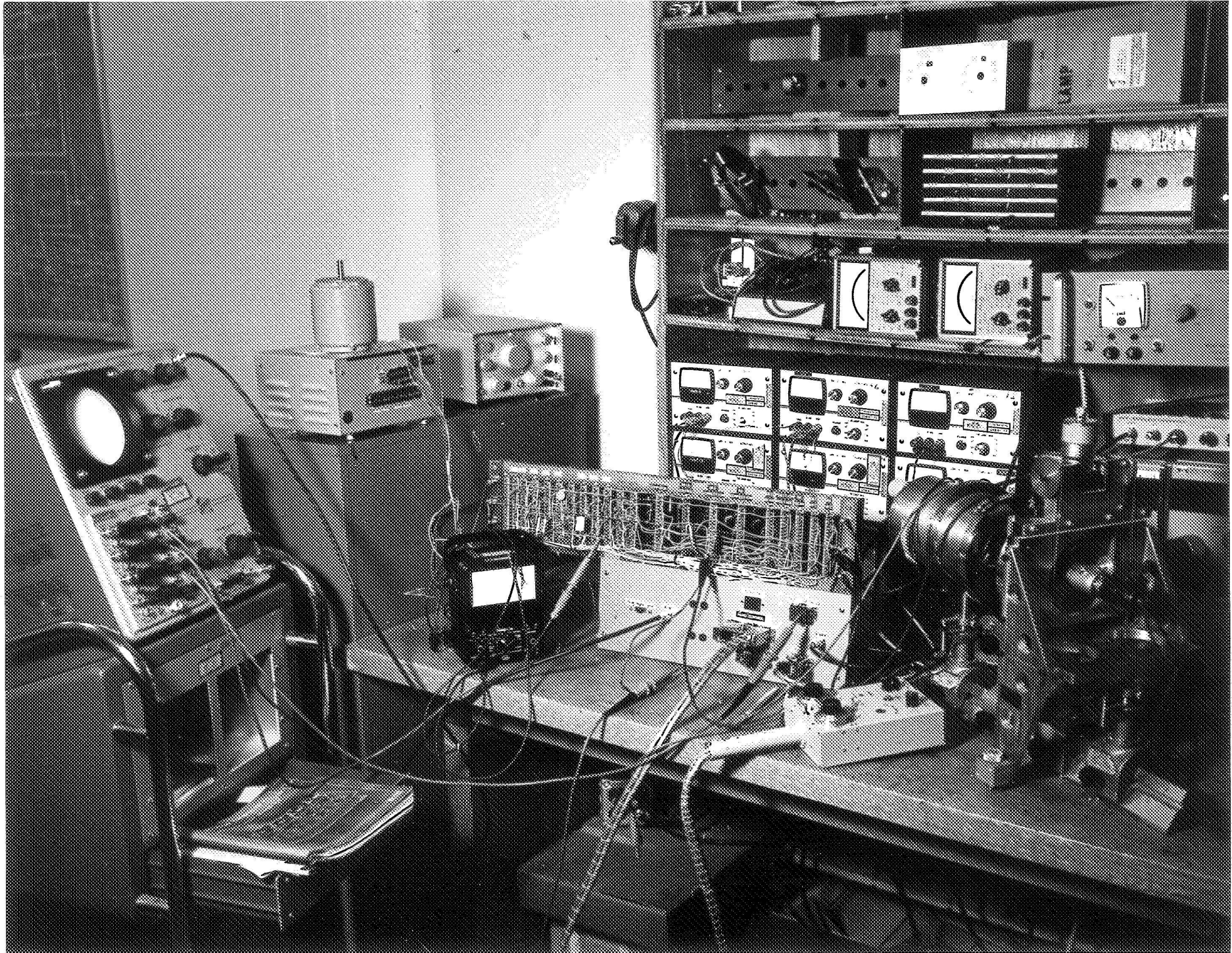


Fig. 1.

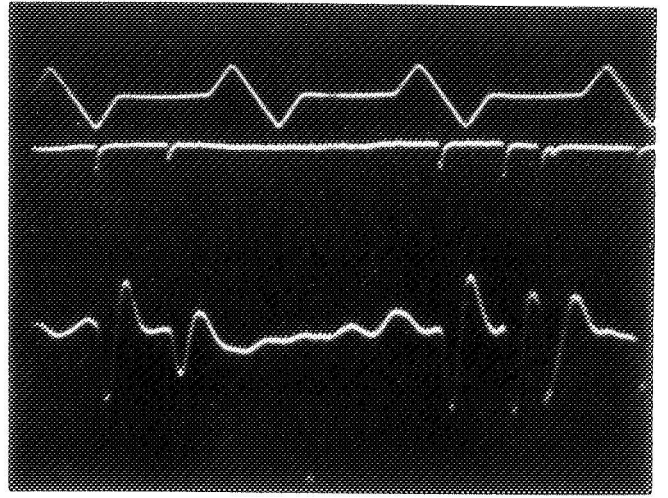
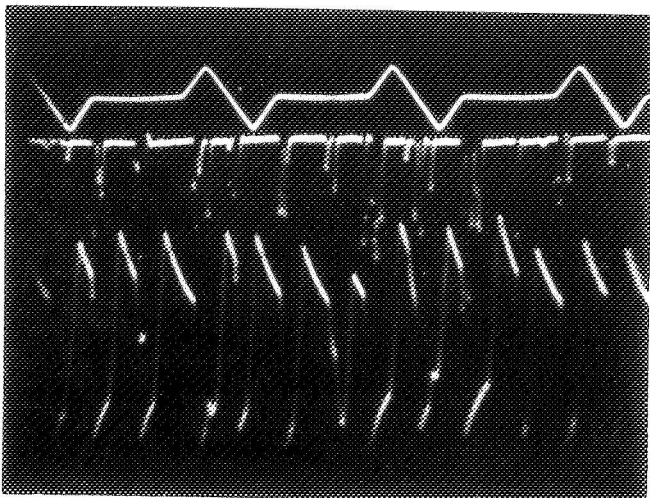
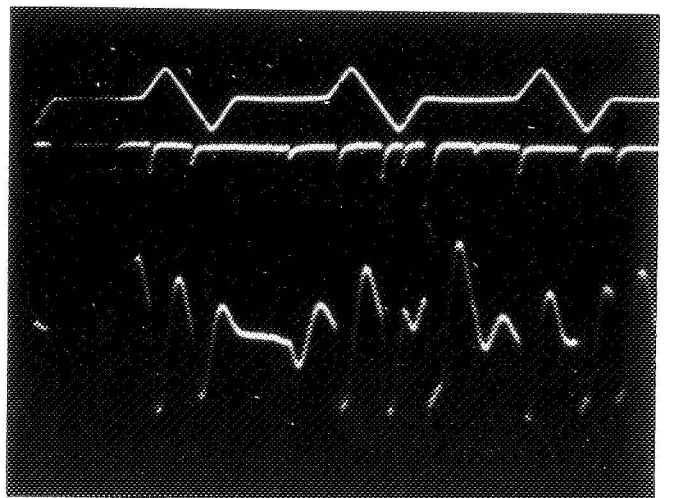
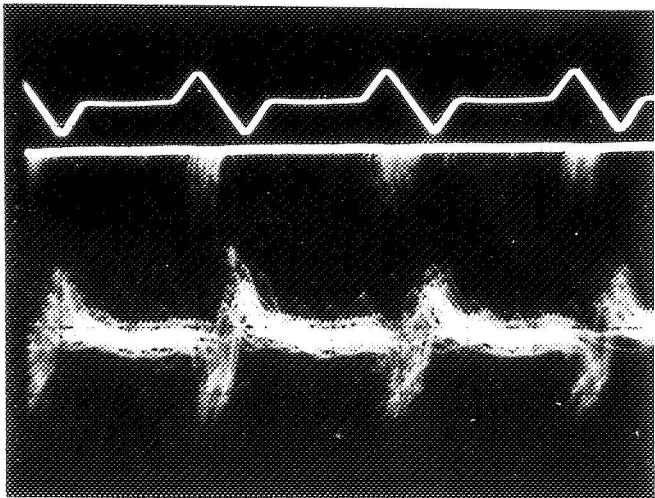
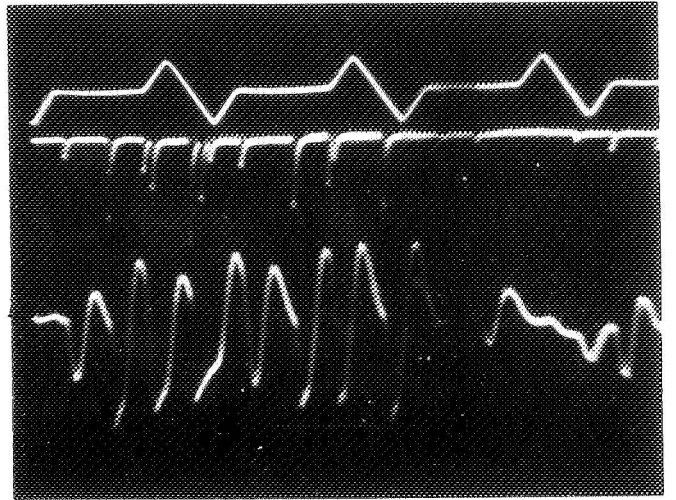
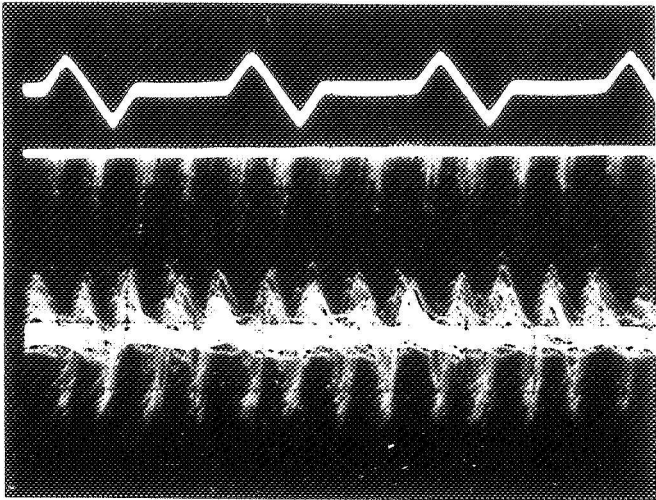


Fig 7.

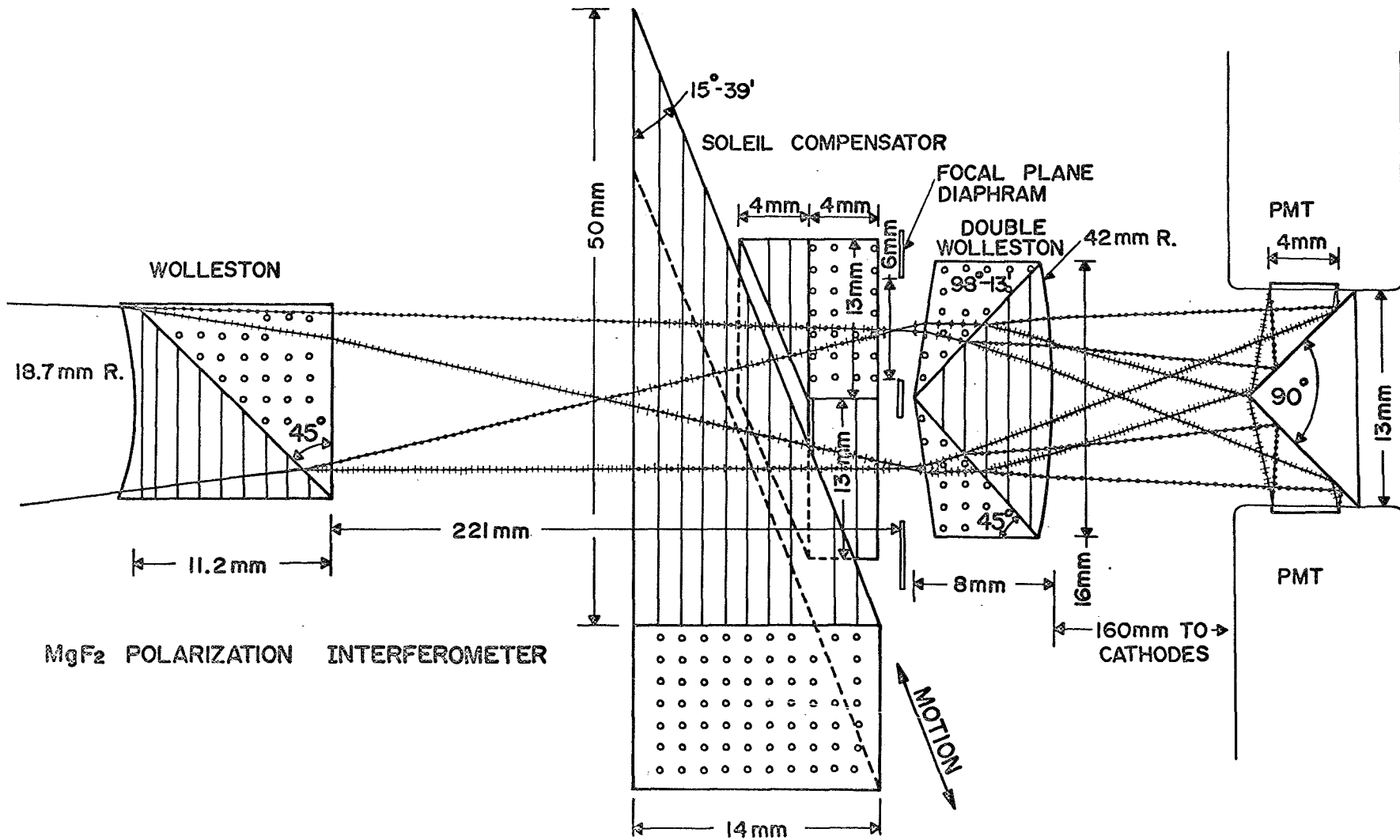
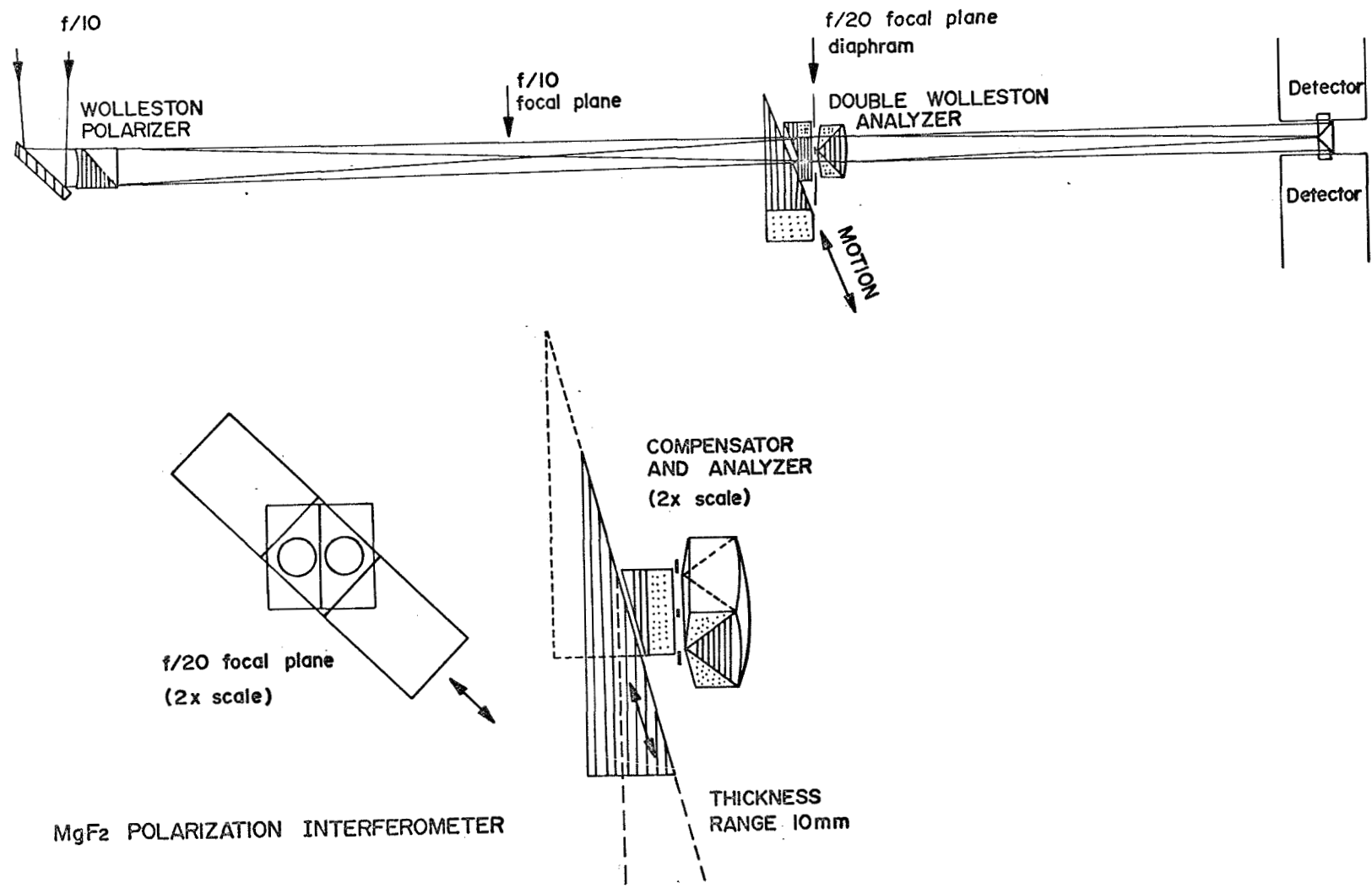


Figure 8a.



MgF₂ POLARIZATION INTERFEROMETER

Figure 8b.

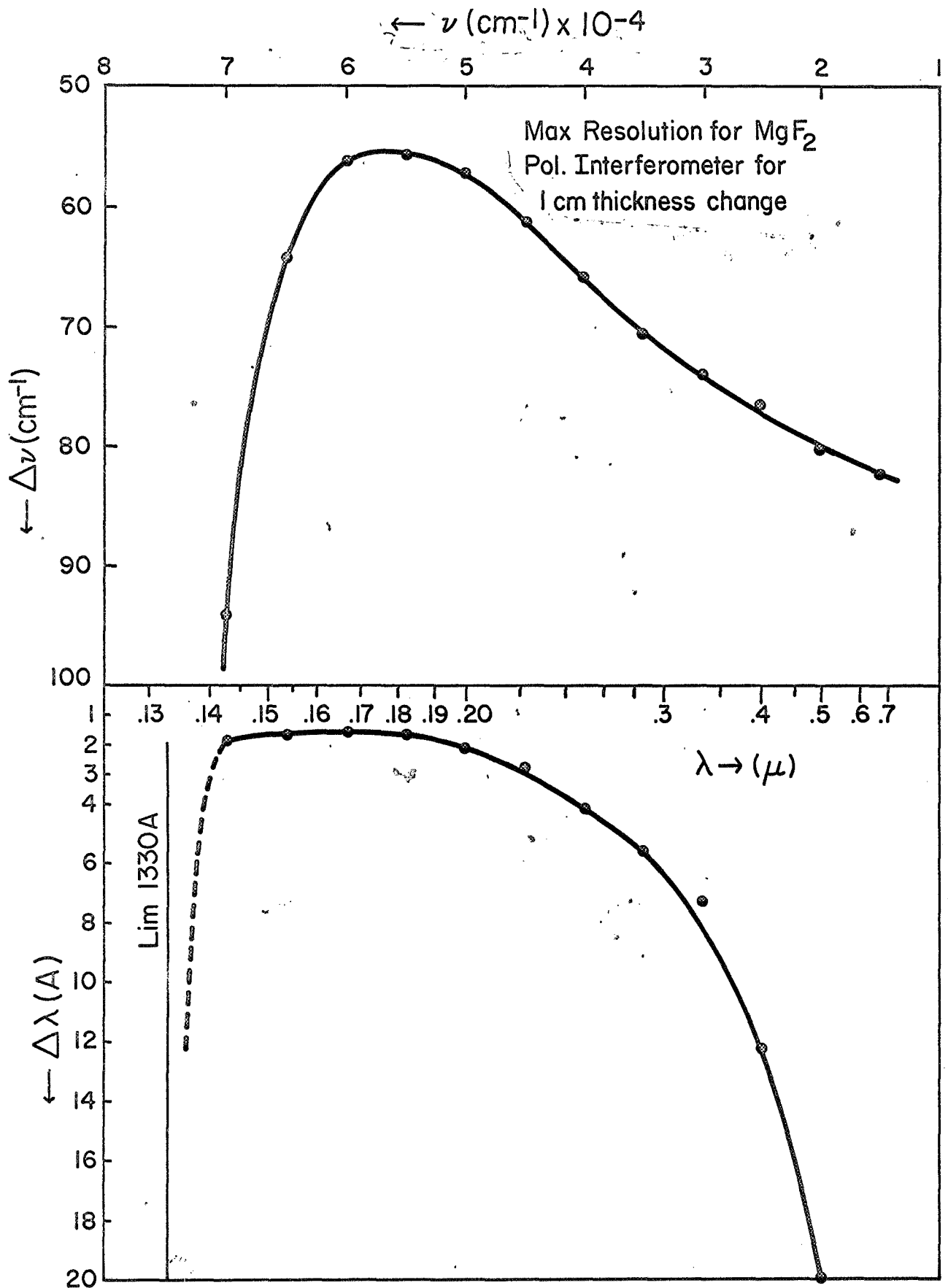


Figure 9.

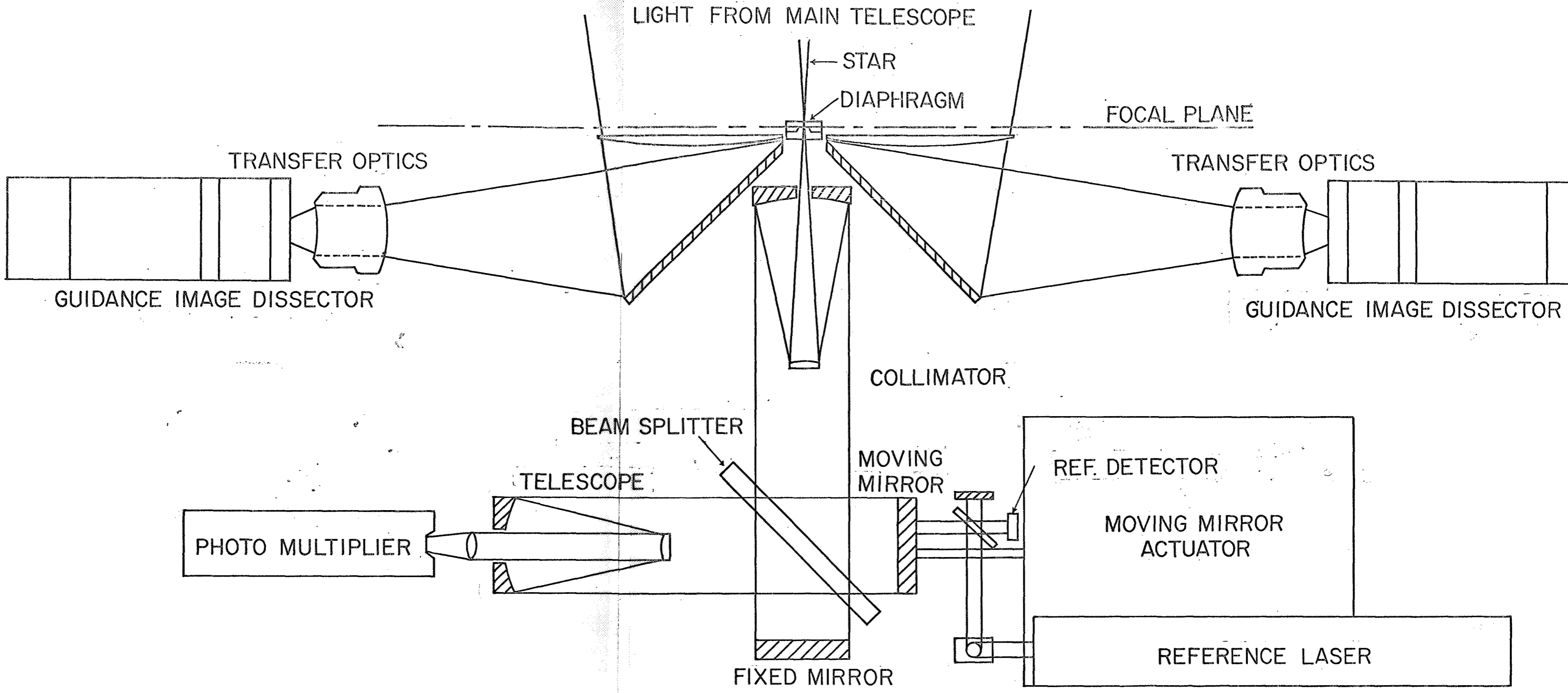


Figure 10.

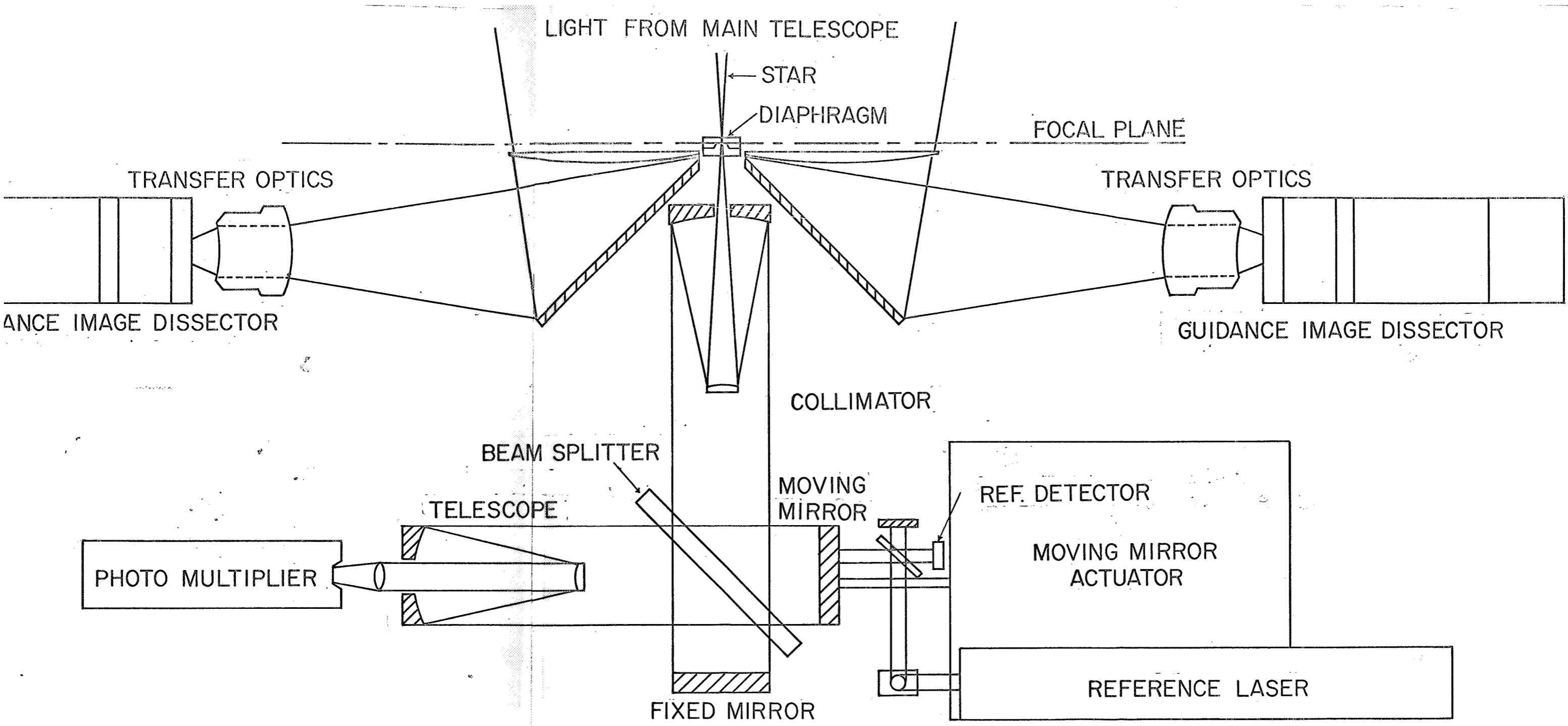


Figure 10.

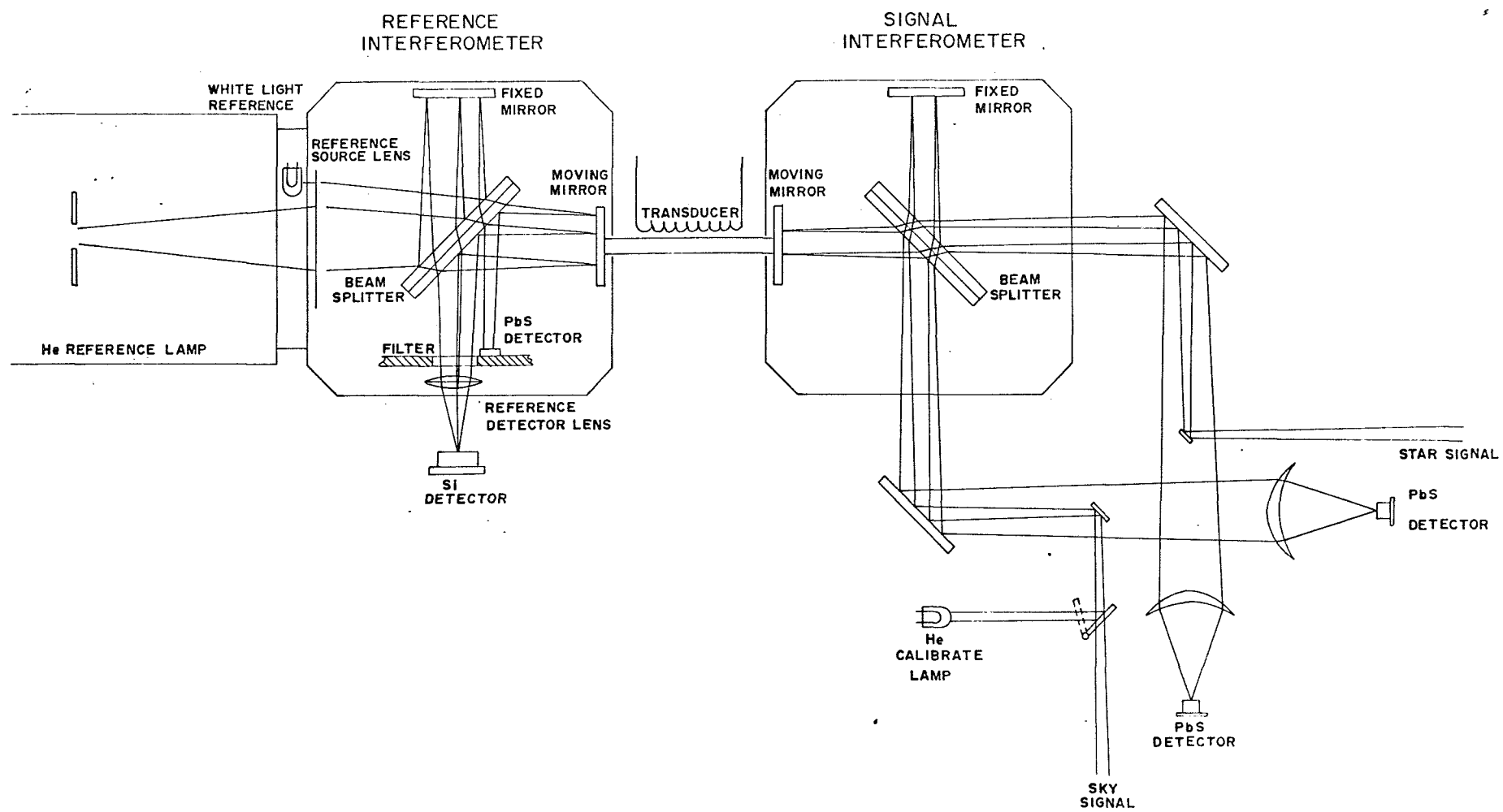


Figure 11.

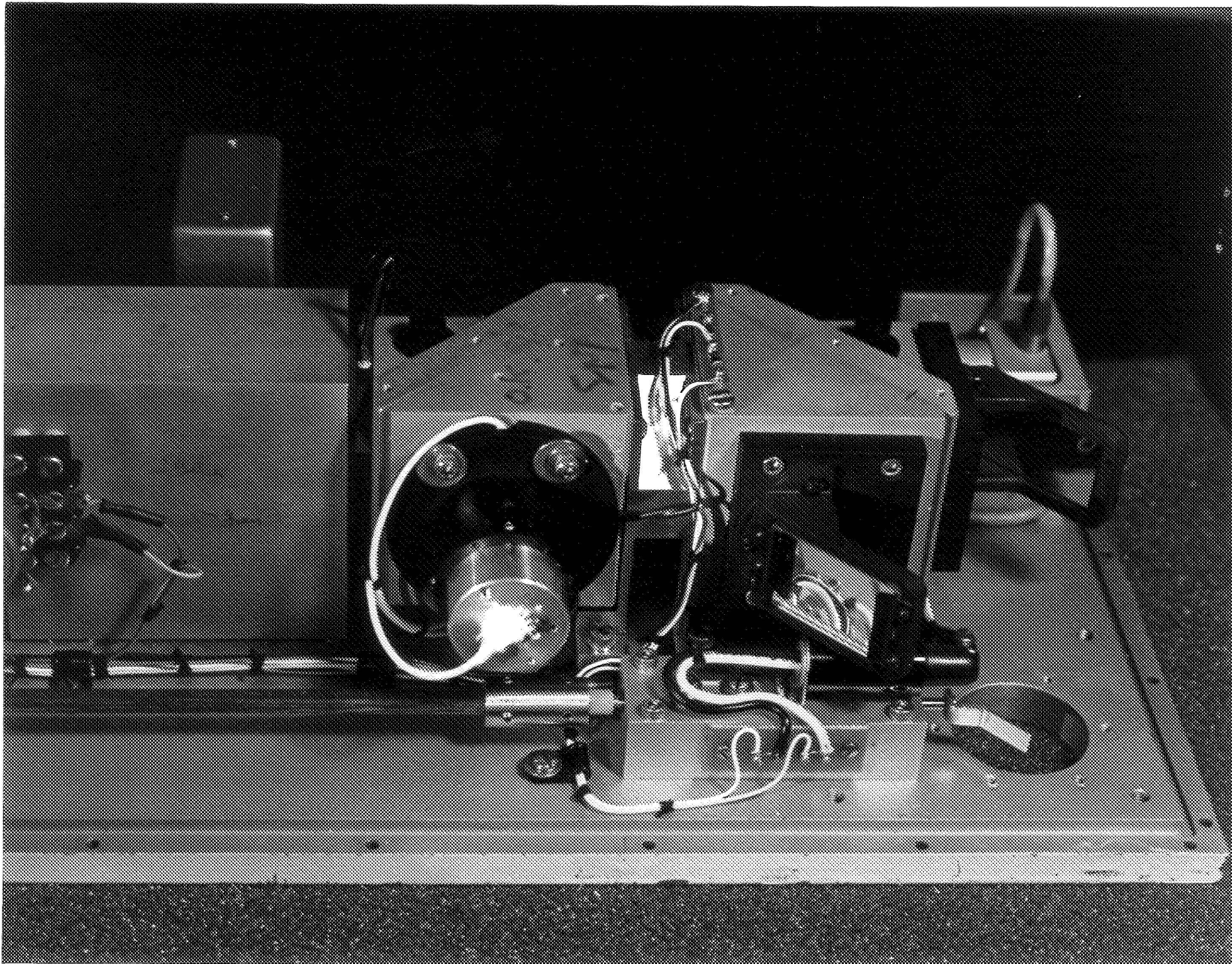


Fig. 12.